Desalination and Water Treatment
www.deswater.com

doi: 10.1080/19443994.2014.981220

57 (2016) 2018–2027
January

Taylor & Francis
Taylor & Francis Group

Selective adsorption of lead (II) ions by a manganese dioxides-loaded adsorption resin

Ying Xiong[a,*], Xuemei Lu[b], Huchun Tao[a]

[a]*Shenzhen Key Laboratory for Metal Pollution Control and Reutilization, School of Environment and Energy, Shenzhen Graduate School, Peking University, Xili University City, Shenzhen 518055, P.R. China, Tel./Fax: +86 755 26032114; email: xiongying@pkusz.edu.cn (Y. Xiong), Tel./Fax: +86 755 26032007; email: taohc@pkusz.edu.cn (H. Tao)*
[b]*China Aerospace Construction Group Limited Company, Haidian District, Beijing 100071, P.R. China, Tel./Fax: +86 10 62754290; email: amanda_vv@163.com*

Received 6 February 2014; Accepted 17 October 2014

ABSTRACT

A new adsorbent SD300-M was successfully synthesized by coating the adsorption resin SD300 with manganese oxide via $KMnO_4$ modification. The results of X-ray photoelectron spectrometer and nitrogen adsorption measurement revealed that the manganese oxide exists as MnO_2 on the surface and inside the channel of the SD300 resin. The SD300-M resin exhibited higher adsorption capacity to Pb^{2+} with the maximum adsorption capacity as high as 141 mg/g, comparing with original SD300 resin and the other manganese oxide-modified adsorbents, such as cellulose or carbon nanotubes. The increased adsorption of Pb^{2+} on the SD300-M resin arose mainly from the formation of inner-sphere complexes with MnO_2. In the presence of Ca^{2+} and Mg^{2+}, the SD300-M resin also has excellent adsorption selectivity for Pb^{2+} relative to that of the D301-M and HMO-001 resins, which arises from electrostatic interaction and surface complexation acting together. All the results indicate that the SD300-M resin is an efficient adsorbent to remove Pb^{2+} from aqueous solution.

Keywords: Selective adsorption; Manganese dioxides; Heavy metals

1. Introduction

Heavy metal pollution in aquatic environments has been given greater attention in recent years. Various kinds of technologies have been used to remove heavy metals from water, such as chemical deposition, membrane separation, biotechnology, adsorption, etc. [1–3]. Among them, adsorption has become the most effective and cost-effective technology, considering the possibility of reuse of adsorbents after desorption and recovery of heavy metals with proper enrichment technology.

Resins have been widely used to treat waters polluted by heavy metals. However, in natural water and industrial wastewater, there are many competing ions, such as alkali metals and alkaline-earth metals coexisting with heavy metals, which make selective adsorption of resins one of the major concerns in the removal of heavy metals in aqueous solution. Efforts have been made to synthesize new resins or to modify existing resins with organic [4] or inorganic compounds [5–10]. Loading metal oxides on adsorbents has proved effective to improve the adsorption and selectivity of heavy

*Corresponding author.

metal ions. Sarkar et al. [9] proposed that resins loaded with hydrous ferric oxide (HFO) successfully produced the commercial resin ArsenX, specifically for the removal of arsenic from aqueous solutions. Pan et al. [5], Zhang et al. [6] and Su et al. [10], however, improved the resin's selectivity for arsenic by loading HFO and for lead by loading hydrous manganese dioxide (HMO) [10].

Manganese oxides not only have a higher affinity for heavy metals compared with Fe or Al oxides [11], but also have good adsorption capacity and selectivity for many heavy metals [11–15]. On the other hand, manganese oxides exist in most cases as fine particles and do not have enough mechanical strength. Therefore, researchers have to resort to other host materials for loading manganese dioxide and to synthesize new adsorbents. These include sand [16], carbon nanotubes [17], bentonite [18], activated carbon [11], zeolite [19,20], cellulose [12], cation-exchange resins [10,21], and anion-exchange resins [13,14,22]. These newly synthesized adsorbents showed excellent adsorption for heavy metals.

Porous ion-exchange adsorbents are regarded as one of the best host materials, because of their potential Donnan membrane effect which allows the charged groups on the matrix to preconcentrate and enhance the metal ions before they are sequestrated by oxide particles [23,24]. However, the charged groups on the matrix react with charged metal ions indiscriminatively by electrostatic action, which decreases the capacity and selectivity of adsorbents for the target metal ions. Therefore, adsorption resins can be regarded as a host material which has neither charged groups on the matrix nor indiscriminate ion exchange actions.

In this study, a new hybrid adsorbent SD300-M was prepared by loading MnO_2 onto the macroporous adsorption resin SD300. Meanwhile, the adsorption behaviors and selectivity of Pb(II) on SD300-M were investigated with fair consideration of varying the pH and competitive adsorption, and the results were compared with the modified anion exchange D301 resin by loading MnO_2, which was termed as D301-M.

2. Materials and methods

2.1. Reagents

All reagents were of analytical grade and purchased from Sinopharm Chemical Reagent Co. Ltd (Beijing, China). The resins used in this research were kindly provided by Zhenguang Resin Co. China. The SD300 resin is an aromatic macroporous adsorption resin with a styrene skeleton and has a brown appearance and a surface area of more than 1,500 m^2/g. The D301 resin is a weak basic, macroporous anion-exchange resin; its principal properties have been documented in the literature [22].

A stock solution of 1,000 mg/L Pb(II) was prepared by dissolving $Pb(NO_3)_2$ in deionized water containing a few drops of concentrated HNO_3 to prevent precipitation of Pb(II) by hydrolysis. The initial pH of the working solution was adjusted by the addition of 0.1 M HNO_3 or 0.1 M NaOH solutions. All solutions were prepared using deionized water.

2.2. Synthesis of adsorbents

Before synthesis, the SD300 resin was purified with absolute alcohol to remove impurities from its synthesis process and then washed with deionized water. The purified resins were dried in the oven at 40℃. One gram of the dry SD300 resin and 100 mL of 0.05 M $KMnO_4$ solution were placed in a beaker. The mixture was shaken for 5 h at ambient temperature, during which the color of the beads changed from brown to black. The synthesis of the MnO_2-loaded resin followed the literature procedures [14,19,20] and the formation of manganese oxide occurs according to the following reaction.

$$2KMnO_4 + 8HCl \rightarrow 2MnO_2 + 2KCl + 3Cl_2 + 4H_2O \quad (1)$$

After filtration, the beads were washed with deionized water to rinse away the excess permanganate ions and nonretained oxides. Then, the black beads were dried at 55℃. The modified resin was named SD300-M meaning beads loaded with manganese dioxide. The resin after adsorbing lead was designated as SD300-MP.

The MnO_2-coated D301 resin (D301-M) was synthesized according to the method proposed in the literature [14,22].

2.3. Resin characterization

The characterizations of the three different resins (SD300, SD300-M, and SD300-MP) were carried out with various methods to indicate the structures and adsorption mechanism of the resins. FT-IR spectra of the samples were obtained by using a Tensor 27 FT-IR spectrometer (Bruker, Germany). X-ray diffraction (XRD) patterns were obtained on a RigakuDmax/2400 X-ray diffractometer. The X-ray photoelectron spectroscopic (XPS) data were taken on an AXIS Ultra instrument from Krators Analytical using the monochromatic Al Kα radiation (225 W, 15 mA, 15 kV) and low-energy electron flooding for charge compensation.

The pore distribution and specific surface areas were measured with a gas adsorption-type porosimeter (Micromeritics ASAP2010, USA).

2.4. Adsorption experiments

In the adsorption study, 0.01 g of an adsorbent was added into 50 mL solution with a Pb(II) concentration of 10 mg/L at various initial pH values (2.0–7.0) to investigate the effects of pH. The flasks were shaken at 140 rpm for 48 h. The pH of the solution was adjusted using 0.1 M HNO_3 or 0.1 M NaOH.

0.010 g of a given adsorbent was introduced into a flask containing 50 mL solution with different concentrations (1, 10, 50, 100, 150, 200, and 250 mg/L) of Pb(II) at pH 5, and shaken at 25°C for 24 h. The Pb(II) concentration of solution was tested before and after the adsorption equilibrium. The experiments were repeated three times and average values were calculated for concentration measurements. All adsorption experiments were duplicated.

For the kinetic experiments, 0.1 g of a specific resin was added into a flask containing 200 mL solution with a Pb(II) concentration of 50 mg/L at pH 5 and shaken at 25°C for 34 h. At various time intervals, 0.5 mL samples were taken. The amount of Pb(II) loaded onto the resins was calculated by conducting a mass balance before and after the test.

The concentrations of Ca^{2+}, Mg^{2+}, Na^{2+}, and Pb^{2+} ion were measured by ICP-OES (Prodigy, Leeman Labs, USA).

3. Results and discussion

3.1. Material characterization

3.1.1. Infrared spectroscopic and XRD analysis

Fig. 1 shows the infrared (IR) spectra of the SD300, SD300-M, and SD300-MP beads. The spectra of three beads were almost same, which indicated that the loading of manganese oxide did not damage the principal structure of the SD300 resin during the synthesis process of the SD300-M resin. There was a new peak at about 520 cm^{-1} appearing in both the SD300-M and SD300-MP spectra, which is attributed to the stretching vibration of the Mn–O bond of the loaded manganese oxides [12,25]. Pb(II) was adsorbed onto the SD300-M resin by ion exchange or adsorption effect without damage to the main structure of the SD300 and the loaded MnO_2 particles.

The XRD pattern of the SD300-M resin (Fig. 2) implied that it was weakly crystallized. There were two weak peaks at about 37° and 66°, which contribute to the crystal structure of manganese dioxide [10,14,26], thus indicating that solid manganese oxides are loaded onto the resin matrix.

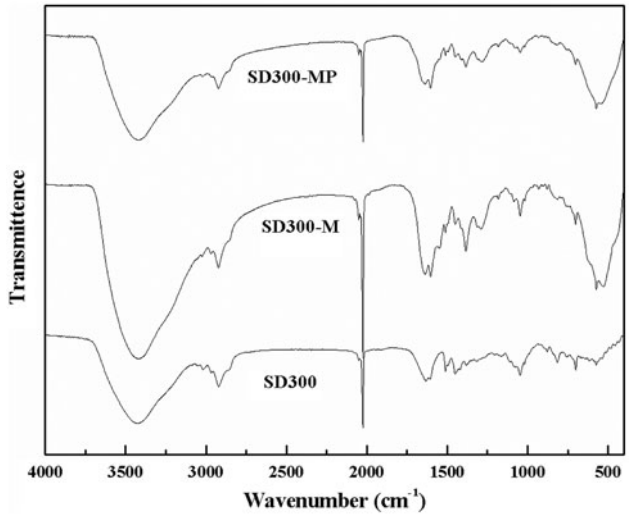

Fig. 1. IR spectra of the SD300, SD300-M, and SD300-MP.

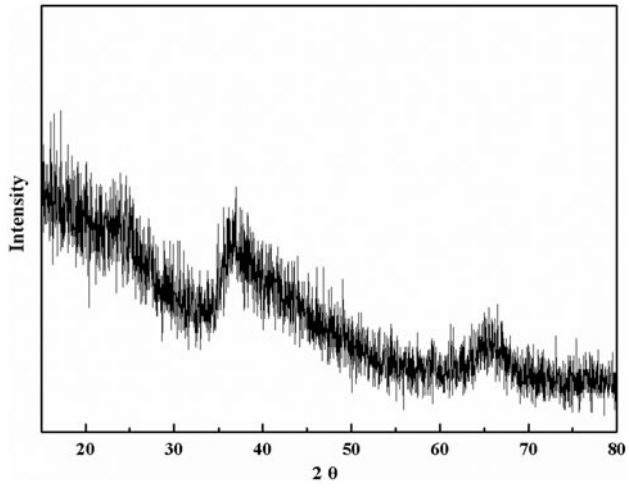

Fig. 2. XRD pattern of the SD300-M resin.

3.1.2. X-ray photoelectron spectroscopic analysis

Fig. 3(a) shows the XPS survey spectra of the SD300, SD300-M, and SD300-MP resins, which indicate clearly the differences of three beads. In order to confirm the Mn oxidation state, detailed scans of the Mn and O regions were performed; the results are shown in Fig. 3(b) and (c). The Mn $2p_{3/2}$ peak is located at 642.24 and 641.95 eV in the SD300-M and SD300-MP resins, respectively, which indicates

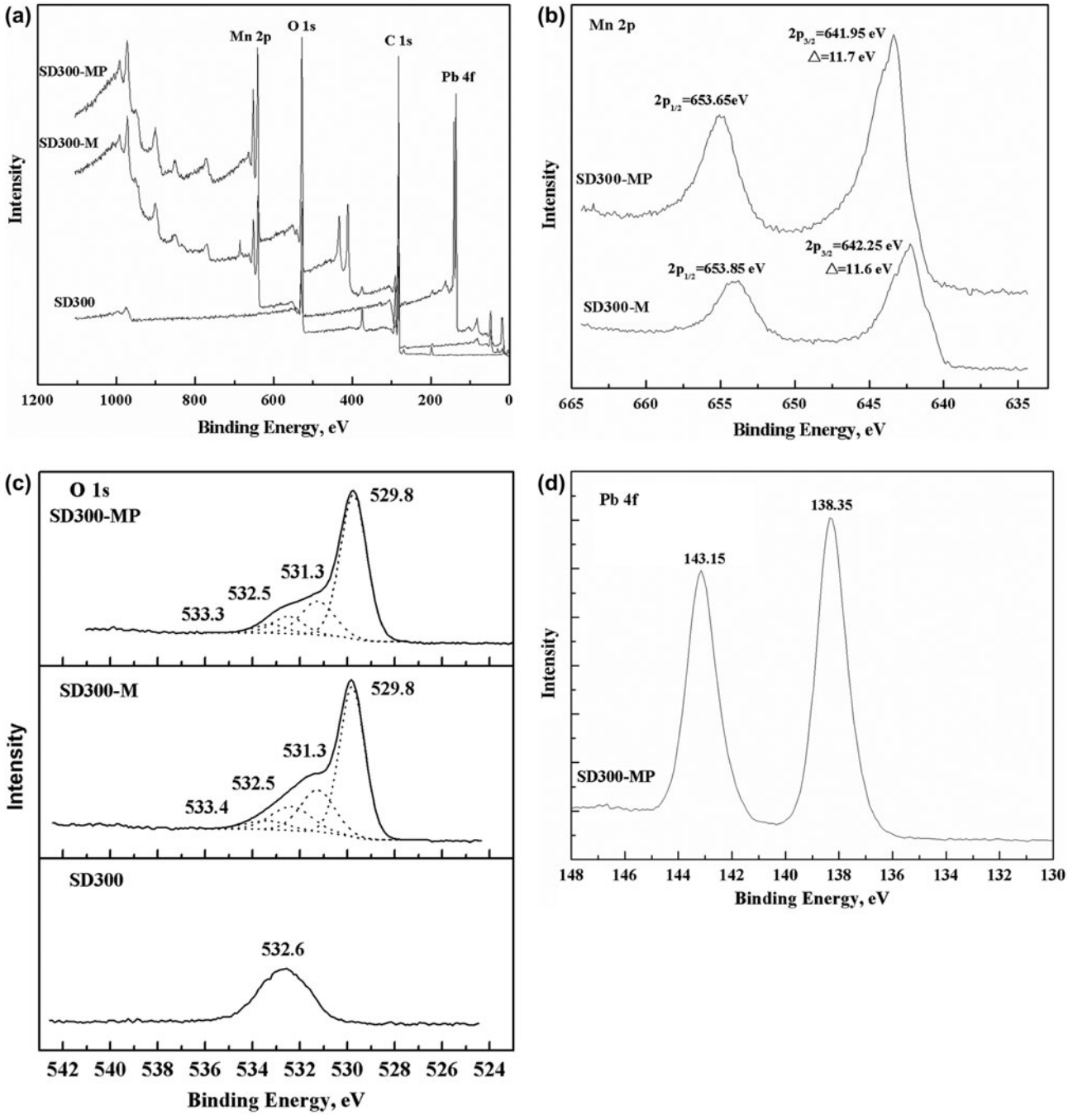

Fig. 3. X-ray photoelectron spectra of the SD300, SD300-M, and SD300-MP beads (a) Survey spectra, (b) Mn 2p spectra, (c) O 1s spectra, and (d) Pb 4f spectra.

that manganese in the loaded manganese oxides is Mn (IV) [12,20,25]. Also, the separations from Mn $2p_{1/2}$ to Mn $2p_{3/2}$ peaks are 11.6 and 11.7 eV in the SD300-M and SD300-MP resins, respectively, which are same as that obtained by Maliyekkal et al. [12], who found that the loaded manganese oxides are MnO_2.

The O 1s peak in the SD300 resin is at the highest binding energy (532.6 eV), which is assigned to a defect oxide, such as O–H, in the main structure of the resin. In the O 1s plots (Fig. 3(c)) of the SD300-M and SD300-MP beads, four oxygen species peaks can be observed. The binding energy of 532.3 and 532.0 eV might be characteristic of oxygen in the principal

Table 1
Textural properties of SD300 and SD300-M adsorbents

Sample	BET (m^2/g)	Micropore area (m^2/g)	Total pore volume (cm^3/g)	Micropore volume (cm^3/g)	Average pore diameter (nm)
SD300	1,292	86.1	0.99989	–	3.095
SD300-M	523.5	177.5	0.44556	0.0639	3.405

structure of the resins as the case in the SD300 resin. The binding energy of 530.9 eV is related to the surface adsorbed OH^-. The binding energy of 529.7 and 529.6 eV can be assigned to the lattice oxygen (Mn–O–Mn) of the loaded MnO_2 [12,20,25]. There was no change in the binding energy of O 1s before and after the SD300-M resin adsorbing Pb(II), which indicated that there was no chemical reaction through the adsorption of Pb(II) onto the SD300-M resin.

Fig. 3(d) shows the Pb 4f spectra of the SD300-MP bead. The peak at a binding energy of 138.35 eV for Pb 4f is characteristic of the Pb–O bond according to the reported literature [12,15]. This confirms that Pb (II) uptake onto the SD300-M resin is mainly due to the formation of inner-sphere complexes. After lead adsorption, the Mn and adsorbed Pb both exist in the SD300-MP bead, which indicates that the loaded Mn atoms in the SD300-M resin do not exist in an ionic state, and the removal of the Pb(II) by the SD300-M resin depends principally on adsorption.

3.1.3. Pore distribution and specific surface area

Before and after synthesis, the pore size and specific surface area of the SD300 and SD300-M resins had changed. Table 1 shows the numerical data for the SD300 and SD300-M resins. The BET and pore volume decreased from 1,292 to 523.5 m^2/g and from 0.99989 to 0.44556 cm^3/g, respectively, after the SD300 resin-loaded MnO_2 particles. These decreases indicate that the deposited MnO_2 is not only on the surface, but also inside the pore channels of the SD300 resin.

The SD300 resin is a macropore resin and the loaded MnO_2 separates the macropores into mesopores or micropores, which leads to an increase in the number of micropores in the SD300-M resin. Hence, compared with the SD300 resin, the micropore area and volume of the SD300-M resin increased and the same results were observed with the MnO_x-loaded biochar [27].

At the same time, the test range of the BET test was set from 1.7 to 70 nm, which is the mesoporous range. The quantity of mesopores in the SD300-M resin increased, and the mean pore diameter increased compared with the SD300 resin.

The nitrogen adsorption–desorption isotherms for SD300-M are shown in Fig. 4, which exhibited an isotherm type IV with a nitrogen hysteretic loop according to the International Union of Pure and Applied Chemistry. The type IV isotherms are given by many mesoporous industrial adsorbents [28]; this implies that the pores of the SD300-M resin are mesoporous.

3.2. Adsorption studies of the SD300-M resin

3.2.1. Effects of pH

The effects of solution pH on Pb(II) removal by the SD300-M and D301-M resins are shown in Fig. 5. For the D301-M resins, the removal rate of Pb(II) increased with increasing pH. The D301 resin is a weak base anion exchange resin. The surface complexation mechanism is involved in the sorption of Pb(II) for the D301-M resins [13].

The Pb(II) removal efficiency of the SD300-M resin increased sharply from 47.9 to 97.0% with the pH rising from 2 to 4. When the pH was between 4 and 6, the percent removal of lead did not change significantly.

Lead adsorption of the SD300 resin was studied for comparison at pH 5 under the same experimental

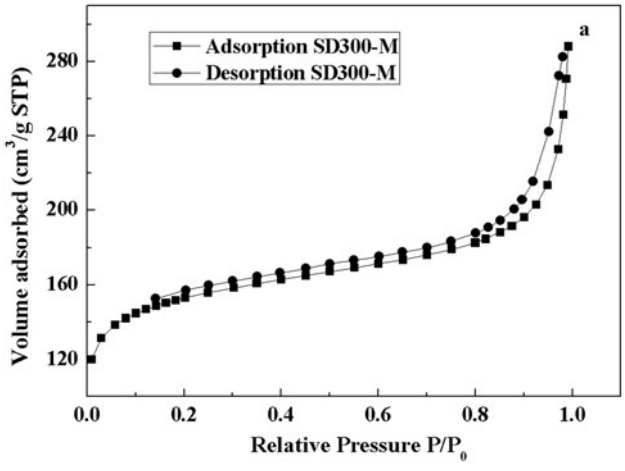

Fig. 4. Nitrogen adsorption–desorption isotherms for the SD300-M resin.

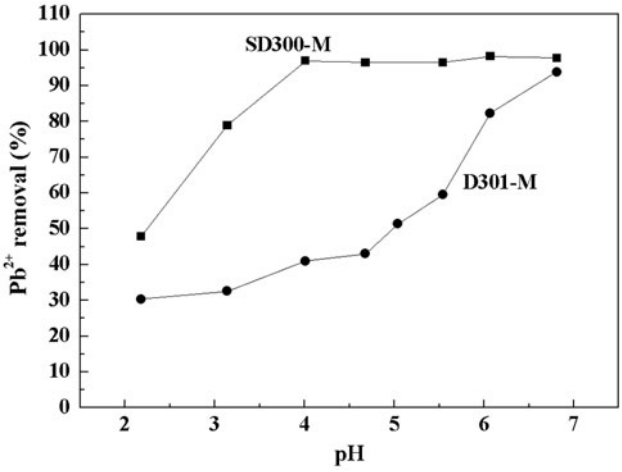

Fig. 5. Effect of pH on the Pb(II) adsorption by the SD300-M and D301-M resins.

conditions. The Pb(II) percent removal with the SD300 resin was only about 1%. The SD300 resin is an adsorption resin, which has no exchangeable ions. This experimental result revealed that the MnO_2 loaded onto the SD300-M resin enhanced the adsorption capacity for Pb(II) ion.

The pH_{pzc} (point of zero charge) of MnO_2 is reported as $1.4 < pH_{pzc} < 4.5$ [29–31]. With increasing pH, the negative charge on the SD300-M surface increases, which enhances the adsorption of Pb^{2+} ions onto the SD300-M resin through electrostatic interaction. When the pH was above 6, the Pb^{2+} percent removal increased mainly depending on the precipitation of Pb^{2+}. Hence, pH 5 was chosen for the following adsorption experiments.

3.2.2. Effect of competitive ions on adsorption

Ca^{2+} and Mg^{2+} ions are normally present in wastewater along with Pb^{2+} ions. When adsorbents are used to remove Pb^{2+} ions, these coexisting ions could occupy the active sites and cause the adsorption of Pb^{2+} to decrease. In order to test the special selectivity of the SD300-M resin to Pb^{2+} in the presence of competing ions, the D301-M resin, which has a good removal effect for Pb^{2+} [13], was chosen for comparison under the same test conditions.

Fig. 6(a) and (b) shows the effect of Mg^{2+} and Ca^{2+} on lead removal by the adsorbents SD300-M and D301-M, respectively. The removal rate of lead by the two adsorbents decreased in the sequence as $Ca^{2+} > Mg^{2+}$, which arises from different hydration energies [10]. Divalent cations with lower hydration energies are adsorbed preferably over those with higher hydration energies. The Gibbs free energy of hydration of these three cations are in the sequence as $Mg^{2+} > Ca^{2+} > Pb^{2+}$, so they give different competing capacities with Pb^{2+}.

The removal rate of Pb(II) by the SD300-M and D301-M resins decreased with increasing concentrations of competitive ions when the initial Ca^{2+} (Mg^{2+})/Pb^{2+} ratio was below 200. But when the ratio increased above 200, the removal rate of Pb^{2+} of the two adsorbents changed only slightly. The SD300 resin is an adsorption resin and has a lower adsorption of lead. The D301-M resin is an anion exchange resin and only can adsorb anions through ionic exchange. So, the excellent adsorption capacity and selectivity of these two modified adsorbents for Pb^{2+} ion come from the loaded MnO_2. It had been reported that lead can form a strong inner-sphere complex with MnO_2 [10,15,32], hence decreasing the effect of the Ca^{2+} and Mg^{2+} competing ions.

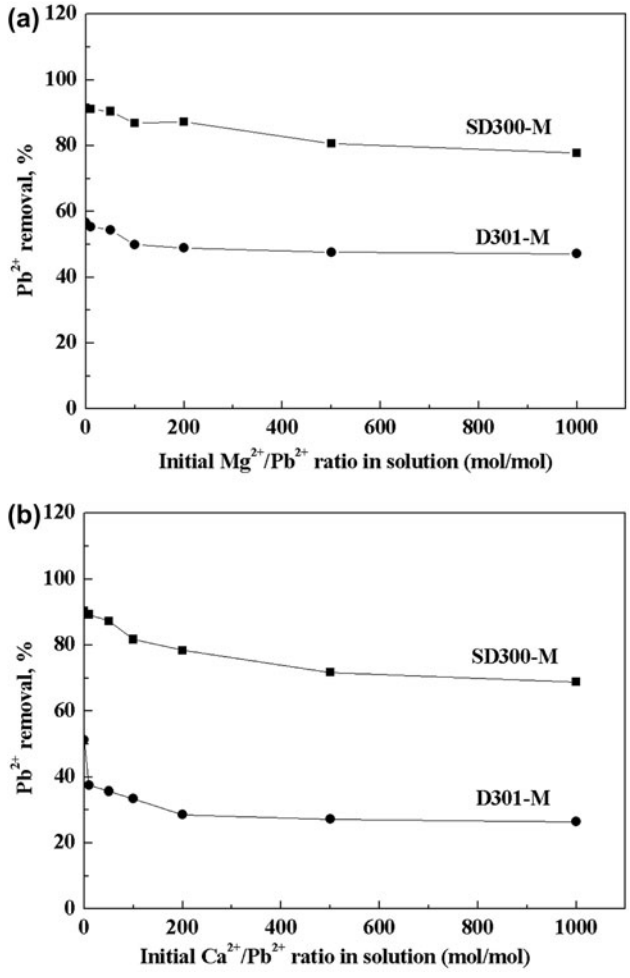

Fig. 6. Effect of (a) Mg^{2+} and (b) Ca^{2+} on lead removal by the D301-M and SD300-M resins at pH 5.0 and 298 K.

The plots in Fig. 6(a) and (b) also indicated that the SD300-M resin has higher adsorption selectivity for lead than does the D301-M resin in the presence of competing cations. This experiment was taken at pH 5. In pH range 5–6, the D301-M surface has a net positive charge, which is unfavorable for adsorption. So, surface complexation was the principal effect for the adsorption of Pb^{2+} on the D301-M resin [13]. In above discussion, the surface of the SD300-M resin had negative charges in pH range 5–6. So for the adsorption of Pb^{2+} onto the SD300-M resin, electrostatic interaction and surface complexation act together.

Compared with the data in the literature [10], the SD300-M resin also had better selectivity than did the HMO-001 resin. The HMO-001 is a new hybrid adsorbent which is fabricated by impregnating nanosized HMO into a porous polystyrene cation-exchange resin (D-001). The adsorption of the HMO-001 resin towards Pb^{2+} is attributed to the host material D001 and HMO particles. But the sulfonic acid groups bound to the D001 matrix preconcentrated the competing cations indiscriminatively at the same time, when it adsorbed Pb^{2+} ions. The host material SD300 resin for the SD300-M resin has no negatively charged groups on the matrix, so it decreased the adsorption of competing cations.

All results indicated that SD300-M resin had excellent adsorption selectivity for lead in the presence of competing ions.

3.2.3. Adsorption equilibrium and kinetics

Normally, Langmuir and Freundlich models have been used to explain the solid–liquid equilibrium for adsorption processes; the corresponding equations are as follows:

$$\text{Langmuir}: \frac{1}{q_e} = \frac{1}{K_L q_m C_e} + \frac{1}{q_m} \tag{2}$$

$$\text{Freundlich}: \ln q_e = \ln K_f + \frac{1}{n} \ln C_e \tag{3}$$

where q_e and C_e are the equilibrium solid-phase (mg/g) and liquid-phase (mg/L) concentrations of Pb^{2+}, respectively, q_m (mg/g) is the maximal adsorption capacity, and K_L (L/mg) is a binding constant in the Langmuir equation. K_f ($mg^{1-n}L^n/g$) is the Freundlich adsorption affinity parameter. Fig. 7 shows lead ion adsorption isotherm of the SD300-M resin at 298 K and Table 2 gives the derived Langmuir and Freundlich constants. It was found that the adsorption of lead on the SD300-M resin fits the Langmuir model very well with a high correlation coefficient $R^2 \geq 0.99$. The maximum adsorption capacity of the SD300-M resin was 140.9 mg/g at 298 K, which is better than other MnO_2-loaded adsorbents, such as C-NMOC

Table 2
Langmuir and Freundlich parameters for lead adsorption onto the SD300-M resin at 298 K

Langmuir equation			Freundlich equation		
q_m (mg/g)	K_L (L/mg)	R^2	n	K_f (L/mg)	R^2
140.9	0.303	0.9938	2.807	0.299	0.9189

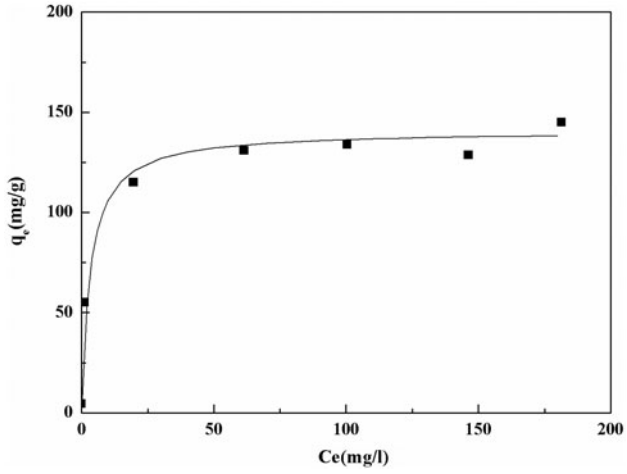

Fig. 7. Adsorption isotherm plot of the SD300-M resin.

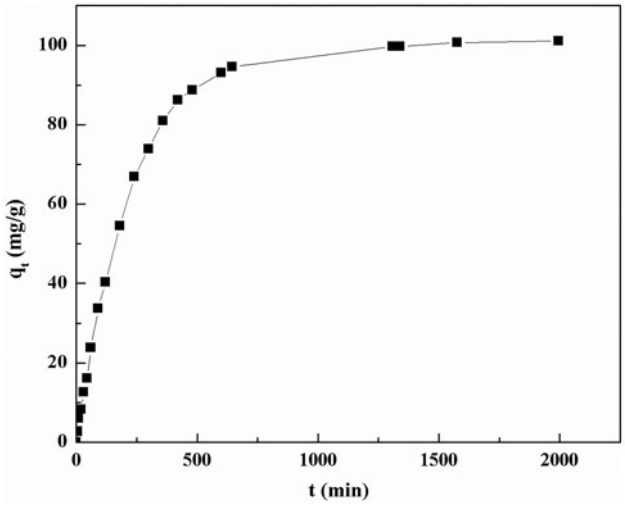

Fig. 8. Adsorption kinetics of Pb^{2+} onto the SD300-M resin at 298 K.

Table 3
Kinetic constants for lead uptake onto the SD300-M resin at 298 K

(a)

	Pseudo-first-order model			Pseudo-second-order model		
q_e (exp.) (meq/g)	k_1	q_e (theor.) (meq/g)	R^2	k_2	q_e (theor.) (meq/g)	R^2
101.1	0.0044	99.95	0.9985	0.000045	113.64	0.9945

(b)

	Intra-particle diffusion model		Liquid film diffusion model	
q_e (exp.) (meq/g)	k_{int} (meq/g $min^{-1/2}$)	R^2	k_1 (meq/g min^{-1})	R^2
101.1	2.6887	0.8456	0.0043	0.9984

(q_m = 75.0 mg/g) [12], MnO_2-loaded D301 resin (q_m = 80.6 mg/g) [13], and MnO_2-loaded carbon nanotube (q_m = 78.7 mg/g) [17]. The Langmuir model is derived based on a monolayer adsorption assumption, so the lead adsorption on the SD300-M resin is likely a monolayer adsorption process.

Fig. 8 shows the lead adsorption kinetics onto the SD300-M resin at 298 K. Four adsorption models were used to interpret the SD300-M adsorption kinetics data: pseudo-first-order, pseudo-second-order, intra-particle diffusion, and liquid film diffusion models, respectively. Table 3(a) and (b) shows the parameters for these four models. The correlation coefficients for the pseudo-first-order model and the liquid film diffusion model ($R^2 > 0.99$) are larger than those for pseudo-second-order model and intra-particle diffusion model. And, the theoretical q_e value (99.95), which was calculated from the pseudo-first-order model also agreed with the experimental q_e value (101.1). These results indicated that the sorption of Pb^{2+} onto the SD300-M resin followed a pseudo-first-order mechanism, likely controlled by physical sorption. And, the liquid film diffusion is the controlling step.

Pseudo-first-order kinetic model:

$$\log(q_e - q_t) = \log q_e - \frac{k_1}{2.303}t \tag{4}$$

Pseudo-second-order kinetic model:

$$\frac{t}{q_t} = \frac{1}{k_2 q_e^2} + \frac{1}{q_e}t \tag{5}$$

Inter-particle diffusion model:

$$q_t = k_{int}t^{0.5} + C \tag{6}$$

Liquid film diffusion model:

$$-\ln\left(1 - \frac{q_t}{q_e}\right) = k_1 t \tag{7}$$

4. Conclusions

A new hybrid absorbent SD300-M resin was synthesized, and its lead adsorption potential was investigated. The XRD, IR, and XPS results indicated that MnO_2 was loaded successfully onto the SD300 resin by *in situ* composition. The results of adsorption equilibrium data fit well to the Langmuir isotherm, and the maximum lead adsorption capacity on the SD300-M resin was 140.9 mg/g at 298 K, which is better than other MnO_2-loaded adsorbents. The lead adsorption on the SD300-M resin was well described by a pseudo-first-order model, and the adsorption was primarily controlled by physical sorption. The SD300-M resin had excellent lead adsorption selectivity in the presence of coexistent Mg^{2+} and Ca^{2+} ions.

Acknowledgments

Financial support from Shenzhen Science and Technology Research Fund Basic Research Program (JC201105170738A) is gratefully acknowledged. The authors are grateful to Prof James R. Bolton from the Department of Civil and Environmental Engineering at the University of Alberta for his kind assistance with our English writing.

References

[1] B.G. Lee, H.J. Lee, D.Y. Shin, Effect of solvent extraction on removal of heavy metal ions using lignocellulosic fiber, Mater. Sci. Forum 486–487 (2005) 574–577.

[2] Q.Y. Chen, Z. Luo, C. Hills, G. Xue, M. Tyrer, Precipitation of heavy metals from wastewater using simulated flue gas: Sequent additions of fly ash, lime and carbon dioxide, Water Res. 43 (2009) 2605–2614.

[3] S. Bouranene, P. Fievet, A. Szymczyk, M.E.H. Samar, A. Vidonne, Influence of operating conditions on the rejection of cobalt and lead ions in aqueous solutions by a nanofiltration polyamide membrane, J. Membr. Sci. 325 (2008) 150–157.

[4] Y.L. Chen, B.C. Pan, H.Y. Li, W.M. Zhang, L. Lv, J. Wu, Selective removal of Cu(II) ions by using cation-exchange resin-supported polyethyleneimine (PEI) nanoclusters, Environ. Sci. Technol. 44 (2010) 3508–3513.

[5] B.C. Pan, Q.J. Zhang, X.Q. Chen, W.M. Zhang, B.J. Pan, Q.X. Zhang, L. Lv, X.S. Zhao, Preparation of polymer-supported hydrated ferric oxide based on Donnan membrane effect and its application for arsenic removal, Sci. China Ser. B: Chem. 37 (2007) 426–431.

[6] Q.J. Zhang, B.C. Pan, W.M. Zhang, B.J. Pan, Q.X. Zhang, H.Q. Ren, Arsenate removal from aqueous media by nanosized hydrated ferric oxide (HFO)-loaded polymeric sorbents: Effect of HFO loadings, Ind. Eng. Chem. Res. 47 (2008) 3957–3962.

[7] B.C. Pan, B.J. Pan, X.Q. Chen, W.M. Zhang, X. Zhang, Q.J. Zhang, Q.X. Zhang, J.L. Chen, Preparation and preliminary assessment of polymer-supported zirconium phosphate for selective lead removal from contaminated water, Water Res. 40 (2006) 2938–2946.

[8] B.C. Pan, Q.R. Zhang, W.M. Zhang, B.J. Pan, W. Du, L. Lv, Q.J. Zhang, Z.W. Xu, Q.X. Zhang, Highly effective removal of heavy metals by polymer-based zirconium phosphate: A case study of lead ion, J. Colloid Interface Sci. 310 (2007) 99–105.

[9] S. Sarkar, L.M. Blaney, A. Gupta, D. Ghosh, A.K. SenGupta, Use of ArsenX^{np}, a hybrid anion exchanger, for arsenic removal in remote villages in the Indian subcontinent, React. Funct. Polym. 67 (2007) 1599–1611.

[10] Q. Su, B.C. Pan, B.J. Pan, Q.R. Zhang, W.M. Zhang, L. Lv, X.S. Wang, J. Wu, Q.X. Zhang, Fabrication of polymer-supported nanosized hydrous manganese dioxide (HMO) for enhanced lead removal from waters, Sci. Total Environ. 407 (2009) 5471–5477.

[11] H.J. Fan, P.R. Anderson, Copper and cadmium removal by Mn oxide-coated granular activated carbon, Sep. Purif. Technol. 45 (2005) 61–67.

[12] S.M. Maliyekkal, K.P. Lisha, T. Pradeep, A novel cellulose-manganese oxide hybrid material by in situ soft chemical synthesis and its application for the removal of Pb(II) from water, J. Hazard. Mater. 181 (2010) 986–995.

[13] L.J. Dong, Z.L. Zhu, H.M. Ma, Y.L. Qiu, J.F. Zhao, Simultaneous adsorption of lead and cadmium on MnO_2-loaded resin, J. Environ. Sci. 22 (2010) 225–229.

[14] V. Lenoble, C. Laclautre, B. Serpaud, V. Deluchat, J.C. Bollinger, As(V) retention and As(III) simultaneous oxidation and removal on a MnO_2-loaded polystyrene resin, Sci. Total Environ. 326 (2004) 197–207.

[15] Q.D. Qin, Q.Q. Wang, D.F. Fu, J. Ma, An efficient approach for Pb(II) and Cd(II) removal using manganese dioxide formed in situ, Chem. Eng. J. 172 (2011) 68–74.

[16] R.P. Han, Z. Lu, W.H. Zou, D.T. Wang, J. Shi, J.J. Yang, Removal of copper(II) and lead(II) from aqueous solution by manganese oxide coated sand: II. Equilibrium study and competitive adsorption, J. Hazard. Mater. 137 (2006) 480–488.

[17] S.G. Wang, W.X. Gong, X.W. Liu, Y.W. Yao, B.Y. Gao, Q.Y. Yue, Removal of lead(II) from aqueous solution by adsorption onto manganese oxide-coated carbon nanotubes, Sep. Purif. Technol. 58 (2007) 17–23.

[18] E. Eren, B. Afsin, Y. Onal, Removal of lead ions by acid activated and manganese oxide-coated bentonite, J. Hazard. Mater. 161 (2009) 677–685.

[19] R.P. Han, W.H. Zou, H.K. Li, Y.H. Li, J. Shi, Copper (II) and lead(II) removal from aqueous solution in fixed-bed columns by manganese oxide coated zeolite, J. Hazard. Mater. 137 (2006) 934–942.

[20] S.R. Taffarel, J. Rubio, Removal of Mn^{2+} from aqueous solution by manganese oxide coated zeolite, Miner. Eng. 23 (2010) 1131–1138.

[21] S.L. Wan, X. Zhao, L. Lv, Q. Su, H.N. Gu, B.C. Pan, W.M. Zhang, Z.W. Lin, J.F. Luan, Selective adsorption of Cd(II) and Zn(II) ions by nano-hydrous manganese dioxide (HMO)-encapsulated cation exchanger, Ind. Eng. Chem. Res. 49 (2010) 7574–7579.

[22] Z.L. Zhu, H.M. Ma, R.H. Zhang, Y.X. Ge, J.F. Zhao, Removal of cadmium using MnO_2 loaded D301 resin, J. Environ. Sci. 19 (2007) 652–656.

[23] F.G. Donnan, Theory of membrane equilibria and membrane potentials in the presence of non-dialysing electrolytes. A contribution to physical–chemical physiology, J. Membr. Sci. 100 (1995) 45–55.

[24] S. Sarkar, A.K. Sengupta, The Donnan membrane principle: Opportunities for sustainable engineered processes and materials, Environ. Sci. Technol. 44 (2010) 1161–1166.

[25] S.H. Liang, F. Teng, G. Bulgan, R.L. Zong, Y.F. Zhu, Effect of phase structure of MnO_2 nanorod catalyst on the activity for CO oxidation, J. Phys. Chem. C 112 (2008) 5307–5315.

[26] M. Villalobos, B. Toner, J. Bargar, G. Sposito, Characterization of the manganese oxide produced by pseudomonas putida strain MnB1, Geochim. Cosmochim. Acta 67 (2003) 2649–2662.

[27] Z.G. Song, F. Lian, Z.H. Yu, L.Y. Zhu, B.S. Xing, W.W. Qiu, Synthesis and characterization of a novel MnOx-loaded biochar and its adsorption properties for Cu^{2+} in aqueous solution, Chem. Eng. J. 242 (2014) 36–42.

[28] K.S.W. Sing, Reporting physisorption data for gas/solid system with special reference to the determination of surface area and porosity, Pure Appl. Chem. 57 (1985) 603–619.

[29] S.S. Tripathy, J.L. Bersillon, K. Gopal, Adsorption of Cd^{2+} on hydrous manganese dioxide from aqueous solutions, Desalination 194 (2006) 11–21.

[30] L. Zhang, J. Ma, M. Yu, The microtopography of manganese dioxide formed in situ and its adsorptive properties for organic micropollutants, Solid State Sci. 10 (2008) 148–153.
[31] R.P. Liu, H.J. Liu, Z.M. Qiang, J.H. Qu, G.B. Li, D.S. Wang, Effects of calcium ions on surface characteristics and adsorptive properties of hydrous manganese dioxide, J. Colloid Interface Sci. 331 (2009) 275–280.
[32] W. Yantasee, C.L. Warner, T. Sangvanich, R.S. Addleman, T.G. Carter, R.J. Wiacek, G.E. Fryxell, C. Timchalk, M.G. Warner, Removal of heavy metals from aqueous systems with thiol functionalized superparamagnetic nanoparticles, Environ. Sci. Technol. 41 (2007) 5114–5119.